Electronic Supplementary Information

Fast cation exchange of layered sodium transition metal oxides for boosting oxygen evolution activity and enhancing durability

Shiyong Chu,[a] Daqin Guan,[a] Hainan Sun,[a] Liangshuang Fei,[a] Zhiwei Hu,[b] Hong-Ji Lin,[c] Shih-Chang Weng,[c] Chien-Te Chen,[c] Ran Ran,[a] Wei Zhou*[a] and Zongping Shao*[ad]

[a]State Key Laboratory of Materials-Oriented Chemical Engineering, College of Chemical Engineering, Nanjing Tech University, Nanjing 210009, P.R. China. E-mail: zhouwei1982@njtech.edu.cn; shaozp@njtech.edu.cn.

[b]Max-Planck-Institute for Chemical Physics of Solids Nöthnitzer Strasse 40, Dresden 01187, Germany

[c]National Synchrotron Radiation Research Center, 101 Hsin-Ann Road, Hsinchu 30076, Taiwan

[d]Department of Chemical Engineering, Curtin University, Perth, Western Australia 6845, Australia

Ⅰ. Experimental

Catalyst Synthesis.

The O3-type $NaCo_{1-x}Fe_xO_2$ (x = 0, 0.2, 0.5, 0.8 & 1) oxides as starting materials for structure re-construction were synthesized by a standard solid-state phase reaction method. The detail synthesis process, taking $NaCo_{0.8}Fe_{0.2}O_2$ as an example, is shown as follows. Firstly, stoichiometric amounts of Co_3O_4 (3.8528 g) and Fe_3O_4 (0.9261 g) were thoroughly mixed with acetone as the liquid dispersant under high-energy ball milling (Fritsch Pulverisette 6) at a rotation speed of 400 rpm for 2 h. After drying, the as-obtained Co_3O_4-Fe_3O_4 mixture (0.2389 g) was further mixed with stoichiometric amount of Na_2O_2 (92.5%, 0.1264 g) in an Ar-filled glove box with the help of an agate mortar and pestle, and then the solid precursors were pressed into a pellet. Then, a few of the same pellets as described above were quickly transferred into high purity oxygen filled quartz tube furnace, followed by high temperature calcination at 650 °C for 12 h to get the final $NaCo_{0.8}Fe_{0.2}O_2$ oxide. Other O3 type $NaCo_{1-x}Fe_xO_2$ oxides were also synthesized via the same process above. The final oxides were directly used, without any purification process.

Electrode Fabrication.

To fabricate the working electrode, 30 μL homogeneous ink containing catalyst, conductive additive and binder was dropped onto hydrophobic carbon paper with a loading area of 0.8 cm^2 and then vacuum dried. In detail, 10 mg catalyst, 10 mg Super P conductive carbon and 250 mL NMP solution 2 wt.% PVDF were dispersed in 850 mL water-free NMP solution for more than 1 h under sonication to form the uniform ink.

Basic Characterizations

Phase structure of the various as-prepared layer-structured oxides was examined by room-temperature XRD (Rigaku Smartlab), and the detail crystal structure parameters were obtained by Rietveld refinement of the XRD patterns based on GSAS program and EXPGUI interface. FE-SEM (Hitachi S-4800) was used to study the micromorphology of the samples. HR-TEM (FEI Tecnai G2 F30 S-Twin) was conducted to obtain the crystal lattice spacing. ICP-AES (Optima 7000DV, Perkin-Elmer, USA) was conducted to obtain the elements compositions of target materials. The catalyst was mixed with KBr to fabricate a disk for the FT-IR (Thermo Nicolet, USA) spectroscopy testing in transmission mode. Quantachrome (AutoSorb-iQ3) nitrogen adsorption-desorption instrument was used to obtain the nitrogen isothermal curves to calculate the S_{BET} of the prepared catalyst. The surface oxygen species of the catalyst was determined by XPS with an Al Kα radiation. XAS was used to obtain the detail oxidation states of the surface and the bulk, and the bond length of the catalyst with the total-electron-yield mode. The SXAS spectra at the Fe-$L_{2,3}$ and the Co-$L_{2,3}$ edges were conducted at BL11A and the Fe-K and Co-K XANES and EXAFS spectra were measured at BL07A of National Synchrotron Radiation Research Center of Taiwan. The EXAFS data were analyzed through Athena software.

Electrochemical Measurements

OER performances evaluation of the catalyst in oxygen saturated 1 $_M$ KOH aqueous solution was conducted by the CHI 760e electrochemistry workstation in three-electrode system at room temperature. For the three-electrode system, the catalyst loaded carbon paper was working electrode, and graphite rod and Ag/AgCl (3.5 $_M$ KCl) were selected as counter electrode and reference electrode. The OER catalytic activity was obtained by linear sweep voltammetry (LSV) polarization plots with a scan rate of 5 mV s^{-1} in the potential range of 0.2-0.8 V (*vs*. Ag/AgCl). Chronopotentiometry (CP) mode was conducted at a current density of 5 mA cm^{-2} to evaluate the catalytic durability of catalysts. The potentials of LSV and CP results were all corrected by *IR* compensation and reversible hydrogen electrode (RHE) correction in this study. Electrochemical impedance spectroscopy (EIS) test of the electrode was performed in 100 kHz - 0.1 Hz.

Ⅱ. Supplementary Results

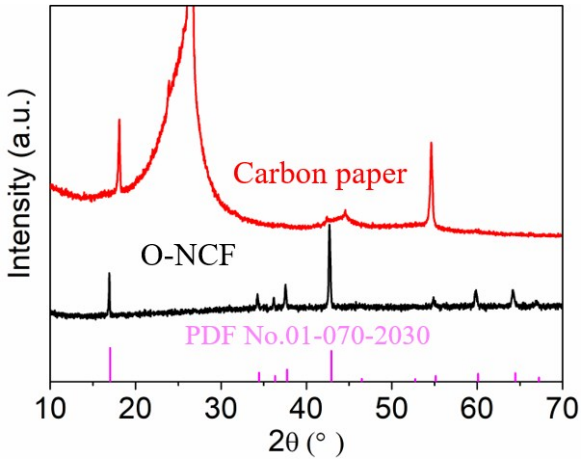

Fig. S1 XRD patterns of O-NCF powder (black line), carbon paper substrate (red line), and the standard XRD pattern (pink line).

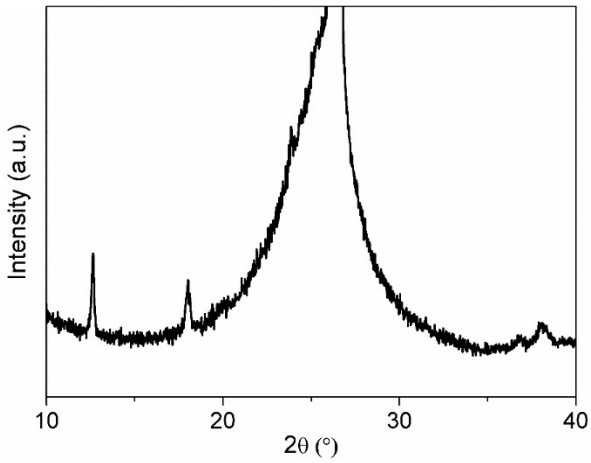

Fig. S2. XRD pattern of O-NCF soaked in 0.1 M HCl for 24 h.

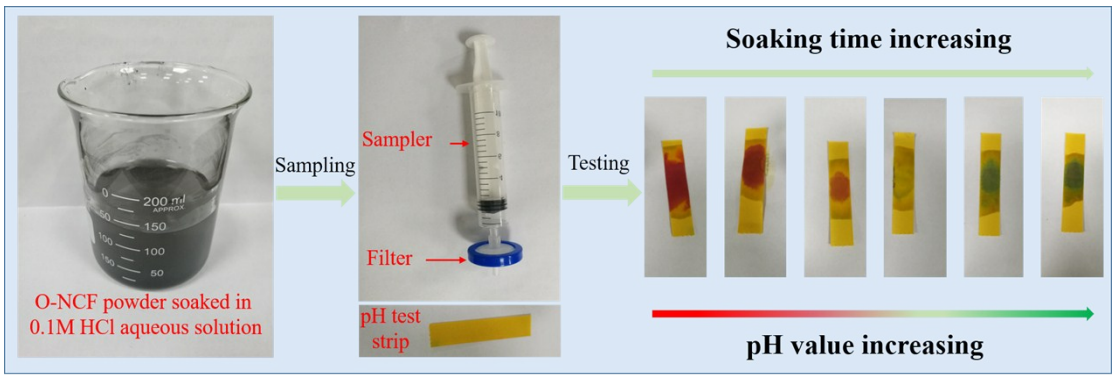

Fig. S3. pH value evolution of 0.1 M HCl aqueous solution under different soaking

time for O-NCF powder.

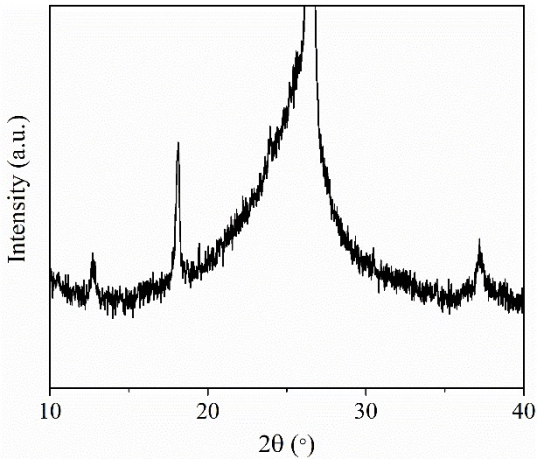

Fig. S4. XRD pattern of O-NCF-OH soaked in 1 M KOH for 2 h.

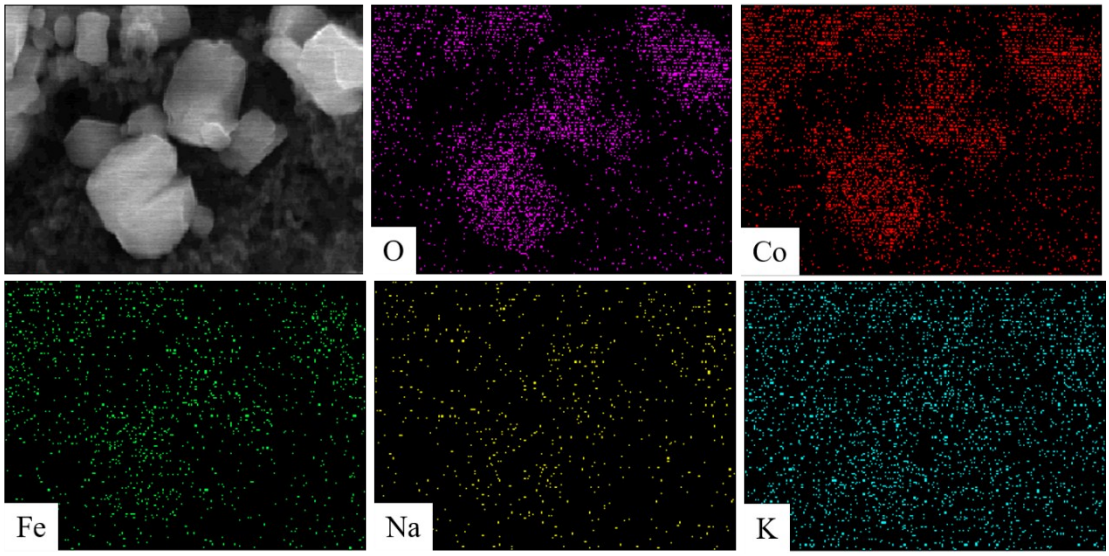

Fig. S5. Elements distribution of O-NCF-OH after a 10-hour chronopotentionmetric testing in 1 M KOH. The elements of Na, Co, Fe and O are uniformly distributed in O-NCF-OH particles, while K shows uniform distribution in the whole screen including the O-NCF-OH particles and the conductive addition of super P. The no aggregation of K in the catalyst suggests no K ion was inserted into the lattice. The sodium ions at the O-NCF-OH near surface/interface have been sufficiently exchanged with hydronium ions, and the 1 M KOH solution is not conducive to the exchange of sodium ions and hydronium ions, so the catalyst after a long-time operation of OER still contains a certain amount of sodium ions, as shown in Fig. S5.

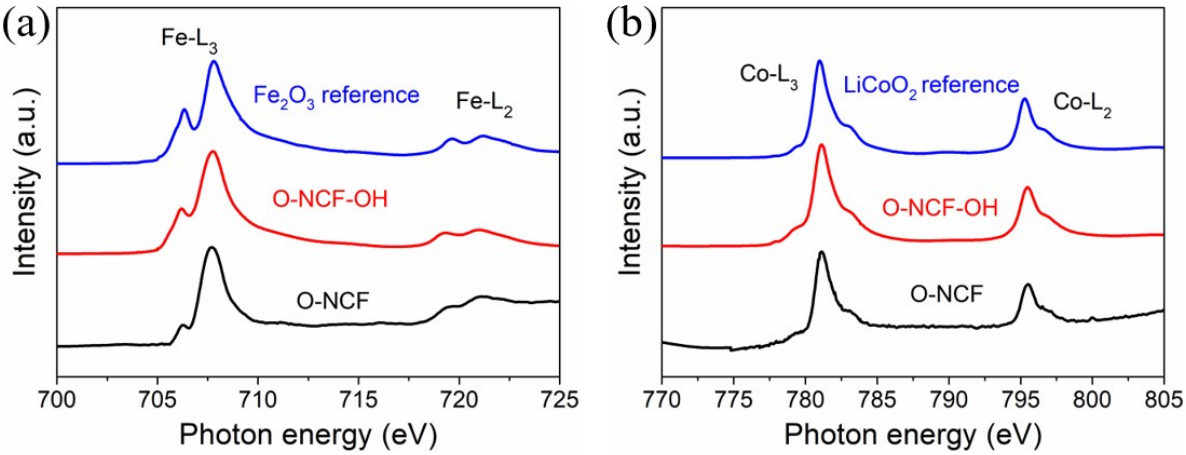

Fig. S6. (a) Fe-$L_{2,3}$ and (b) Co-$L_{2,3}$ XAS spectra of O-NCF and O-NCF-OH and of Fe_2O_3 and $LiCoO_2$ as Fe^{3+} and Co^{3+} references.

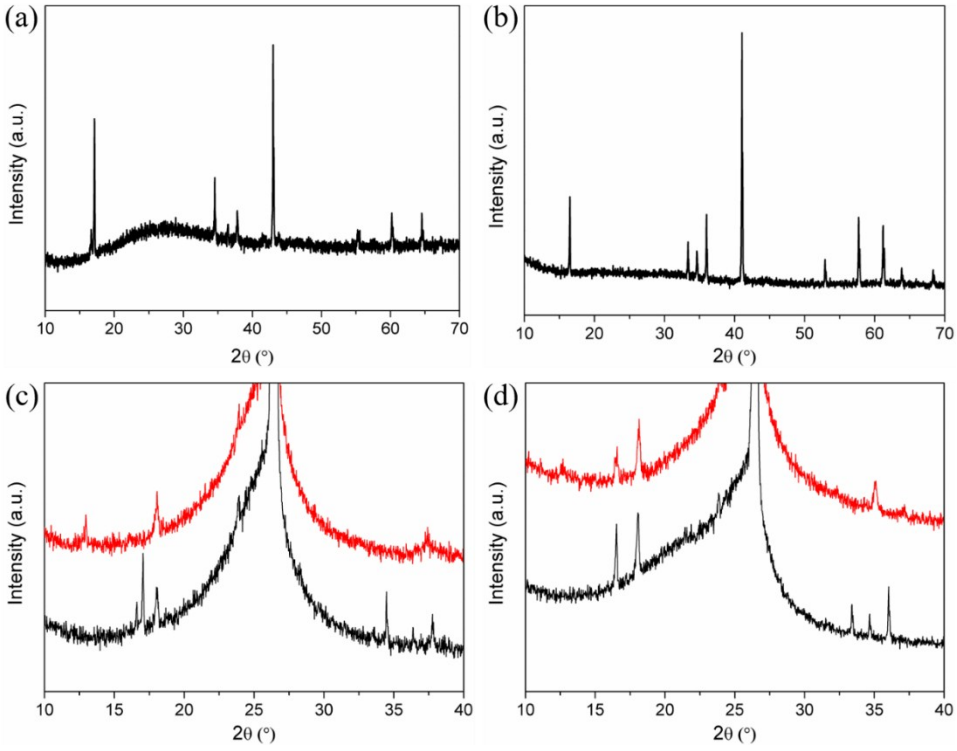

Fig. S7. XRD patterns of O3 phase (a) $NaCoO_2$ and (b) $NaFeO_2$ powder. XRD patterns of carbon paper supported (c) $NaCoO_2$ and (d) $NaFeO_2$ soaked in 0.1 M HCl with 0 min (black curves) and 10 min (red curves).

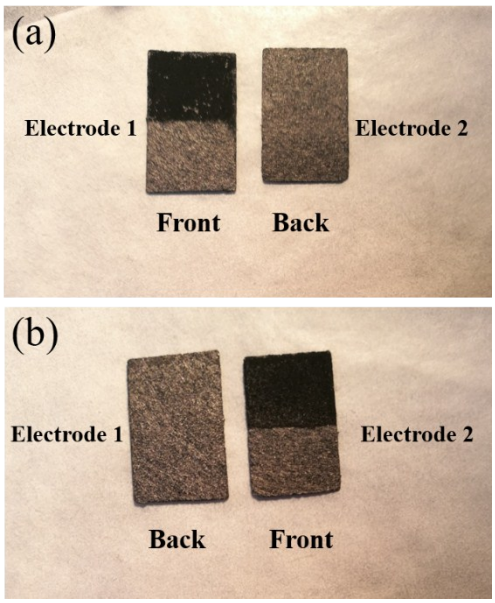

Fig. S8. Digital photos of O-NCF electrodes. a) The front of electrode 1 and the back of electrode 2. b) The back of electrode 1 and the front of electrode 2.

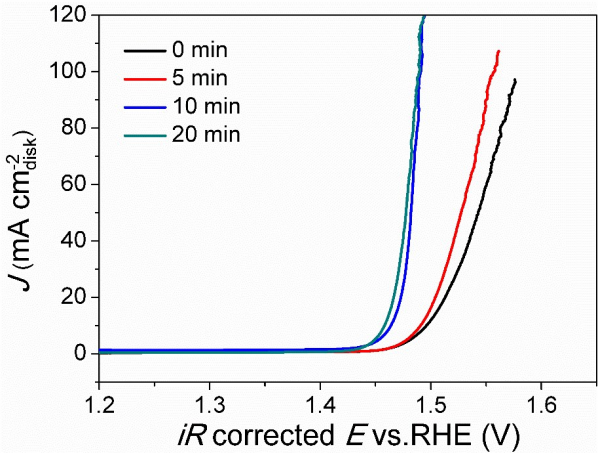

Fig. S9. LSV polarization curves of O-NCF with different soaking time in 0.1 M HCl.

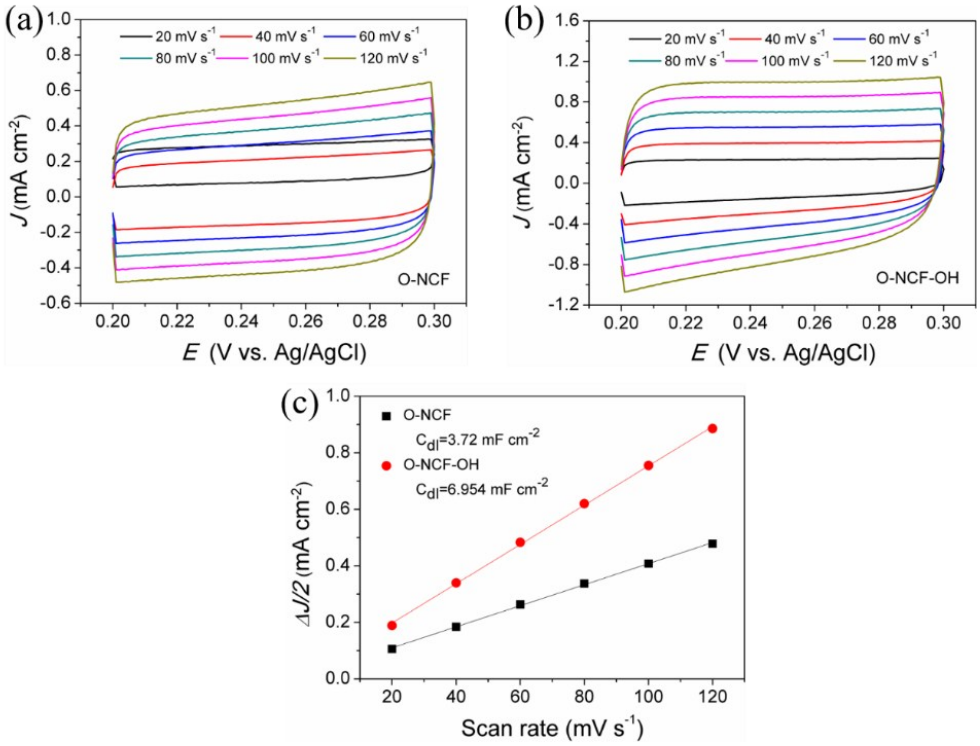

Fig. S10 CV plots of (a) O-NCF and (b) O-NCF-OH electrodes at different CV sweep speeds (20, 40, 60, 80, 100, and 120 mV s^{-1}). (c) Linear fit curves of capacitive currents vs. different CV sweeping speeds (20, 40, 60, 80, 100, and 120 mV s^{-1}) of O-NCF and O-NCF-OH.

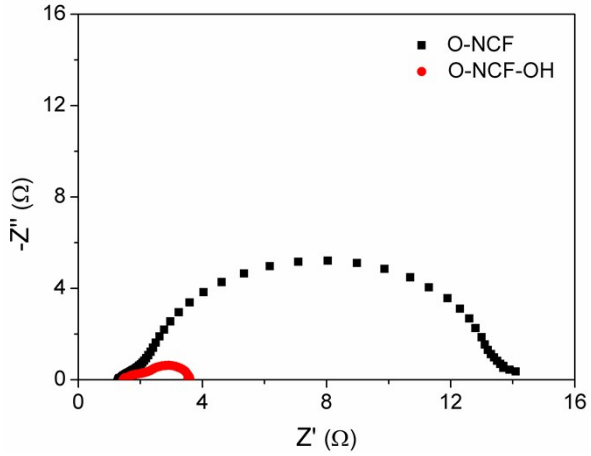

Fig. S11. EIS curves of O-NCF and O-NCF-OH electrodes.

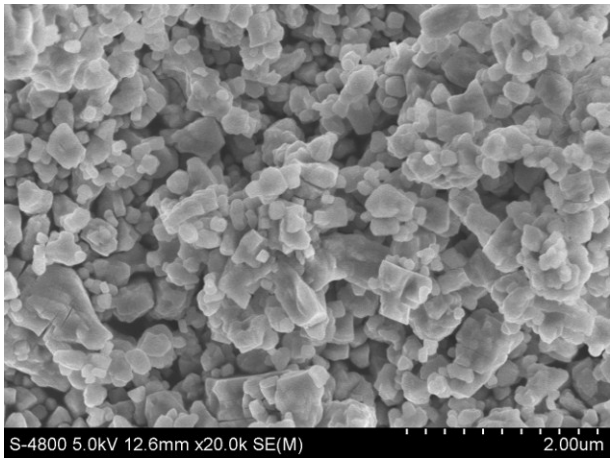

Fig. S12. SEM image O-NCF-OH.

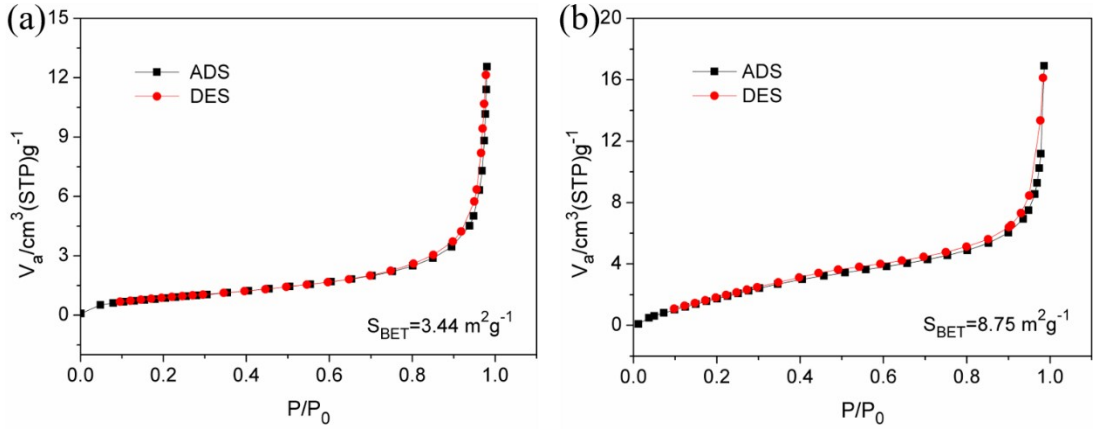

Fig. S13. N_2-isothermal adsorption-desorption curves of (a) O-NCF and (b) O-NCF-OH.

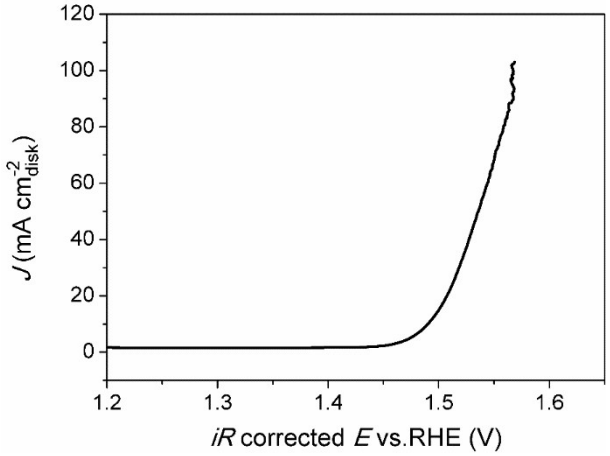

Fig. S14. LSV polarization curve of vacuum dried O-NCF-OH.

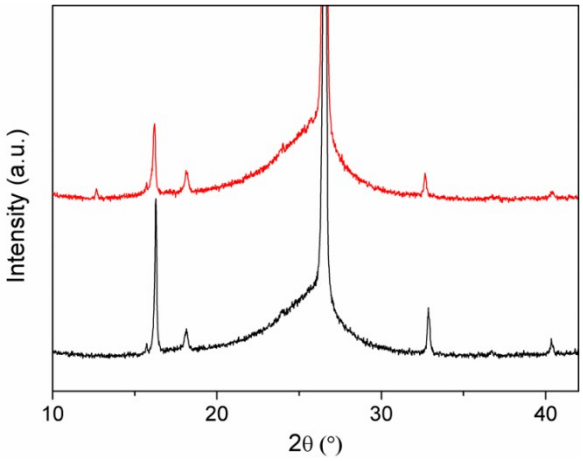

Fig. S15. XRD patterns of pristine P2 phase P-NC (black curves) and 0.1 M HCl aqueous solution soaked P-NC (red curves), namely P-NC-OH.

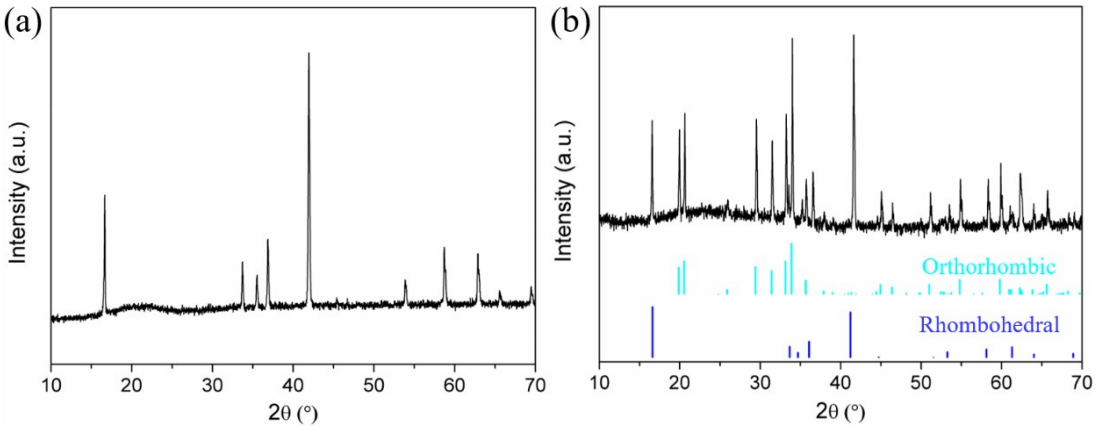

Fig. S16. XRD patterns of O3 phase a) O-NCF-55 and b) O-NCF-28 powder. O-NCF-28 was consisted of rhombohedral (PDF No. 01-087-0274) $NaCo_{1-x}Fe_xO_2$ ($x > 0.5$) and orthorhombic (PDF No. 01-080-1159) $NaFeO_2$.

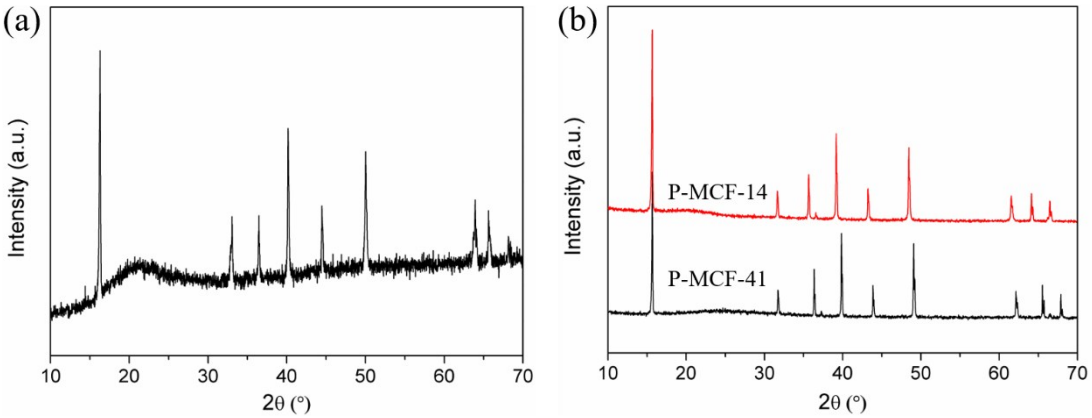

Fig. S17. (a) XRD patterns of P2 phase P-NC. (b) XRD patterns of P2 phase P-MCF-41 (black curve) and P-MCF-14 (red curve).